Localization of Inelastic Tunneling and the Determination of Atomic-Scale Structure with Chemical Specificity

B. C. Stipe, M. A. Rezaei, and W. Ho
Laboratory of Atomic and Solid State Physics and Center for Materials Research, Cornell University, Ithaca, New York 14853

(Received 18 September 1998)

The orientation of individual C_2HD molecules adsorbed on the Cu(100) surface at 8 K was determined from inelastic tunneling images obtained with a scanning tunneling microscope. The simultaneously recorded constant-current images showed that the deuterium end of the molecule appears 0.006 Å lower than the hydrogen end, which was further substantiated by quantitative measures of the molecular rotation. Extension of the study to C_2HD on Ni(100) revealed that the orientation of the molecule relative to the molecule's shape in the constant-current images contrasts sharply between the two surfaces. [S0031-9007(99)08530-0]

PACS numbers: 68.35.Ja, 07.79.Cz, 34.50.Ez, 61.16.Ch

Atomic-scale structure is traditionally determined by averaging over large homogeneous samples using diffraction or spectroscopy methods. X-ray crystallography and nuclear magnetic resonance are among the most powerful of these methods. In contrast, the scanning tunneling microscope (STM) is capable of producing real-space atomic-resolution images of a wide range of samples including DNA [1] and can determine the chirality of individual molecules [2]. However, the atomic-scale features in STM images can be difficult to predict [3] and tip dependent [4]. A major drawback of the STM is a lack of chemical specificity as a result of the broad spectroscopic structure and complexity of the electronic density of states involved in tunneling. It has recently been demonstrated, however, that the STM is capable of vibrational spectroscopy [5] in a manner analogous to traditional inelastic electron tunneling spectroscopy (IETS) [6]. By combining the spectroscopic resolution of IETS with the atomic-scale spatial resolution of STM, we demonstrate how atomic structure may be determined in real space with chemical specificity.

Experiments were conducted with a homemade variable-temperature STM in ultrahigh vacuum (UHV) [7]. The Cu(100) and Ni(100) samples were cleaned by ion sputtering and annealing cycles. To reduce carbon contamination, the Ni(100) surface was oxidized at room temperature with oxygen and reduced by annealing in hydrogen. Polycrystalline tungsten STM tips were also cleaned by several ion sputtering and annealing cycles in UHV. The sample and microscope were cooled to 8 K for the experiments. The surface was then exposed to acetylene until a coverage of ~0.001 monolayer was observed in STM images.

Vibrational excitation of the molecule occurs when tunneling electrons have enough energy to excite a quantized vibrational level. An ac modulation was added to the sample bias voltage, V, and the resulting tunneling current, I, was fed into a lock-in amplifier to detect the first and second harmonics of the modulation frequency [5,7]. These harmonics are proportional to dI/dV (the ac tunneling conductance) and d^2I/dV^2, respectively. To obtain an inelastic tunneling image, the dc bias voltage was set to match a vibrational energy. As the tip was scanned across the surface, the STM feedback loop was periodically turned off and the modulation voltage turned on to record the second harmonic signal.

The adsorption of acetylene on Cu(100) and Ni(100) has been studied extensively by traditional diffraction and spectroscopy techniques. On Cu(100), the near-edge x-ray-absorption fine structure (NEXAFS) has shown the C-C bond to be parallel to the surface and significantly stretched [8]. Interpretation of NEXAFS data suggests that the C-H bonds bend away from the surface [9]. The mirror planes of acetylene on Ni(100) have been determined by angle-resolved electron-energy-loss spectroscopy (EELS) [10] and are consistent with the C-C bond adsorbed diagonally on the fourfold hollow site [11]. This site and orientation have also been suggested for acetylene on Cu(100) based on the similarities between the EELS spectra on these two surfaces [12]. The symmetry in STM images of acetylene on Cu(100) confirms adsorption across the diagonal of the fourfold sites [5]. However, the presence of two mirror planes in the images is consistent with the orientation of the C-C bond along either diagonal. In the vibrational imaging experiments presented in this paper, the site and orientation of acetylene on both Cu(100) and Ni(100) are unambiguous. The results for Cu(100) are, however, in disagreement with the adsorption sites and orientations determined previously by NEXAFS [9,13].

The acetylene isotopes C_2H_2, C_2D_2, and C_2HD appear to be the same in STM images (Fig. 1a) but can be easily identified from their vibrational spectra (Figs. 1b and 1c), where the characteristic C-H and C-D stretch energies are observed. The C-H stretch vibrational energies are in good agreement with EELS for C_2H_2 on Cu(100) [12] and Ni(100) [10]. For C_2D_2, the C-D stretch energy is consistent with the expected isotopic shift. For the singly deuterated species, C_2HD, the detection of C-H and C-D stretches shows single bond sensitivity for STM-IETS. Small upward shifts in the C-H and C-D stretch energies are

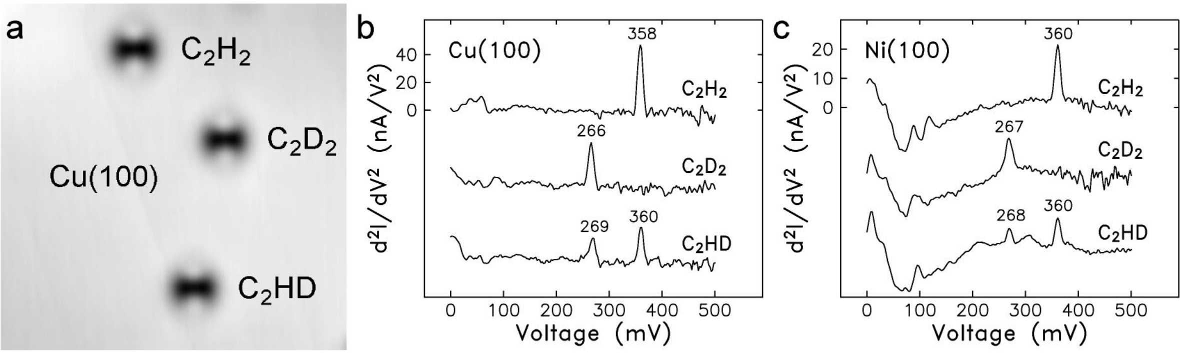

FIG. 1. STM image (a) and single-molecule vibrational spectra (b) of three acetylene isotopes on Cu(100) at 8 K. The vibrational spectra on Ni(100) are shown in (c). The imaged area in (a), 56 Å × 56 Å, was scanned at 50 mV sample bias and 1 nA tunneling current. Inelastic tunneling spectra in (b) are the average of 16 scans of 2 min each while the vibrational spectra in (c) are the average of 25, 50, and 222 scans for C_2H_2, C_2D_2, and C_2HD, respectively. Background spectra over the bare surfaces have been subtracted. A rms modulation voltage of 5 mV at 200 Hz was used. The tip was positioned over the center of the molecule in the recording of the spectra and was fixed in position vertically to give a dc tunneling current of 1 nA at 249 mV sample bias.

observed for this species and are more pronounced on Cu than Ni. The magnitude of the changes in tunneling conductance across the peaks are tip dependent. For acetylene on Cu(100) and the specific case shown in Fig. 1b, the conductance changes are 12.7%, 9.2%, 4.9%, and 5.8% for C_2H_2, C_2D_2, C-D in C_2HD, and C-H in C_2HD, respectively. The corresponding conductance changes for acetylene on Ni(100) (Fig. 1c) are 6.9%, 3.9%, 1.6%, and 3.0%, respectively. The intensity ratio of the C-D to C-H peaks is $\sim$0.7 on Cu(100) and $\sim$0.55 on Ni(100). This dependence of the inelastic tunneling signal strength on the reduced mass of the oscillator is in good agreement with one-dimensional resonant scattering models [14,15].

By setting the sample bias voltage to the corresponding vibrational energy of the C-D stretch mode in C_2HD on Cu(100), and simultaneously recording both the STM image and the vibrational image, the spatial distribution of the C-D stretch signal within the molecule can be determined (Figs. 2a and 2b). The maximum in the C-D inelastic tunneling channel occurs 1.2 Å from the molecule's center. Because this is near the midpoint of the C-D bond, the inelastic imaging appears to locate the position of the bond in this case. The molecule has four equivalent orientations separated by 90° within the fourfold site. With sufficient tunneling voltage and current, the molecule can be rotated [16] until a rescan verifies a total rotation of 180° (Figs. 2c and 2d). Subtraction of Fig. 2c from Fig. 2a reveals an asymmetry of the C_2HD molecule in the constant-current STM images (Fig. 2e). Comparison to the vibrational images shows that the deuterium side of the molecule appears $\sim$0.006 Å lower than the hydrogen side in the STM image. Maximum contrast is located 2.8 Å away from the molecule's center. The asymmetry is also evident in images recorded at much lower bias voltages ($<$50 mV). Because this voltage is below the onset of the various inelastic tunneling channels (including the bending modes), the asymmetry is evidently a result of purely elastic tunneling.

The asymmetry may be a result of anharmonicity of the potential energy well; the higher zero-point energies of the vibrational modes (bending and stretch) involving H relative to those involving D would then result in a greater average displacement from the minimum of the well. The mean C-H bond length in CH_4 has been determined to be longer than the mean C-D bond length in CD_4 by at most 0.003 Å [17].

The asymmetry of C_2HD in STM images could also be a result of the contraction of the electron wave functions around the deuteron. One can understand the physical origin of this contraction by considering the simple case of H and D ground state wave functions which fall off as e^{-r/a_0}, where a_0 is the Bohr radius of H or D. The increase in the reduced mass of the electron in D, μ_e, affects its wave function since $a_0 = \hbar^2/\mu_e e^2$. For a STM tip located at $r \sim 6$ Å away, one would expect a height difference in STM images of 0.002 Å. A more realistic modeling of both the density of electronic states above C_2HD and the zero-point motions involving H and D is necessary to fully account for the 0.006 Å height difference seen in Fig. 2e.

The vibrational images in Figs. 2b and 2d show that the spatial distribution of the inelastic tunneling is well localized to the chemical bond being probed. Further evidence of this localization was obtained from the statistics of molecular rotation induced by the tunneling electrons as a function of the tip position relative to the molecule. The rotation rate of acetylene on Cu(100) increases dramatically when the C-D (in C_2D_2) or C-H (in C_2H_2) mode is excited [16]. Rotation is induced when the C-D or C-H stretch excitation decays. The rotation rate is therefore proportional to the inelastic tunneling signal, and the spatial dependence of the rotation rate can be used to produce the same information as the inelastic tunneling images. More specifically, the statistics of C_2HD rotation can reveal the molecule's asymmetry. The tip was positioned at a fixed distance (2 Å) perpendicular to the plane of the molecule (as determined from the vibrational images) before the feedback was turned off and the voltage was increased to 300 mV. Individual rotation events are observed as sudden changes in the tunneling current (Fig. 3a). From the vibrational images, low current corresponds to the orientation with the tip outside the plane of the molecule while high current corresponds to the orientation with the tip inside the plane of the molecule. The distribution of rotation times for the low current state is an exponential distribution (Fig. 3b). At 300 mV, the C-D mode is excited while the C-H mode is not (Fig. 1b). As one might expect from the spatial localization of the inelastic tunneling (as deduced from the vibrational images), the molecule rotates much (~10 times) faster when the C-D bond is under the tip than when the C-H bond is under the tip. This can be seen in the double-exponential distribution of rotation times for the high current state (Fig. 3c). Close examination of the tunneling current in Fig. 3a also shows that the current is slightly lower when the deuterium is under the tip than when the hydrogen is under the tip. Calibration of I versus tip displacement shows that the observed current difference (0.7 nA or 1.7%) would result in a 0.007 Å tip displacement if the STM feedback loop was on. This agrees well with the value (0.006 Å) found from the STM images (Fig. 2e).

The distributions of rotation times for C_2HD on Ni(100) (Figs. 3d and 3e) show that the rotation rates are ~100

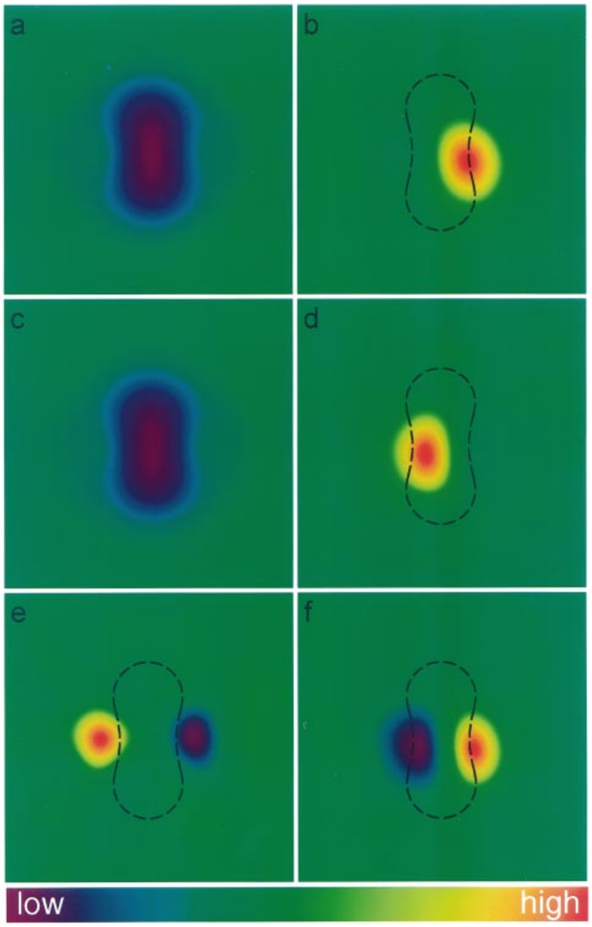

FIG. 2(color). Spatial mapping of the inelastic tunneling signal. Singly deuterated acetylene (C_2HD) on Cu(100) was imaged in constant-current mode (a) simultaneously with the vibrational (d^2I/dV^2) image (b) at 269 mV. The vibrational image shows the intensity distribution of the C-D stretch relative to the depressed part of the conventional STM image (dashed outline). No contrast in vibrational images was observed for bias voltages more than ~10 mV away from 269 mV. The corresponding images for the rotated molecule [(c) and (d)] are subtracted and shown in (e) and (f). All image areas are 17 Å × 17 Å and were scanned at a dc tunneling current of 1 nA. The vibrational images were obtained with a rms modulation voltage of 10 mV at 200 Hz. Images are the average of 2 scans of 6 min each and have been subjected to a low-pass filter to remove high frequency noise.

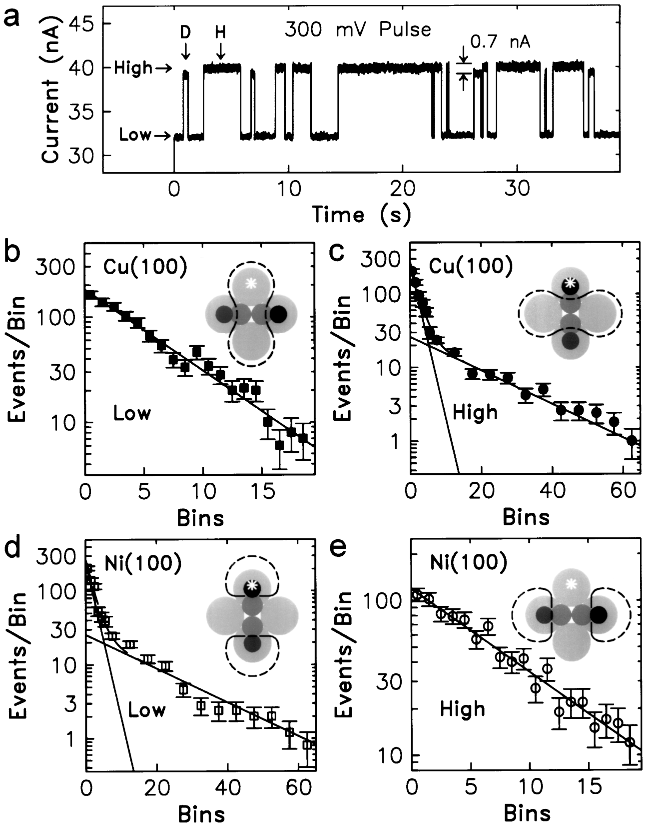

FIG. 3. Distributions of single-molecule rotation times for C_2HD. An example of the tunneling current during a 300 mV pulse on Cu(100) is shown in (a). Distributions of rotation times are shown for the low (b) and high (c) current states. Distributions for Ni(100) are shown in (d) and (e). In the schematic insets, the position of the tip is marked with an asterisk while the depressed part in STM images is outlined. The bin widths are 100 ms in (b) and (c), and 1 ms in (d) and (e). Bins have been averaged in groups of five in the tails of the distributions of (c) and (d). The analysis includes a total of 4041 single-molecule rotation events. The probabilities of rotation per tunneling electron are (b) 9.5×10^{-12}, (c) 2.0×10^{-11} (fast), 2.1×10^{-12} (slow); (d) 2.7×10^{-9} (fast), 2.9×10^{-10} (slow); and (e) 6.4×10^{-10}.

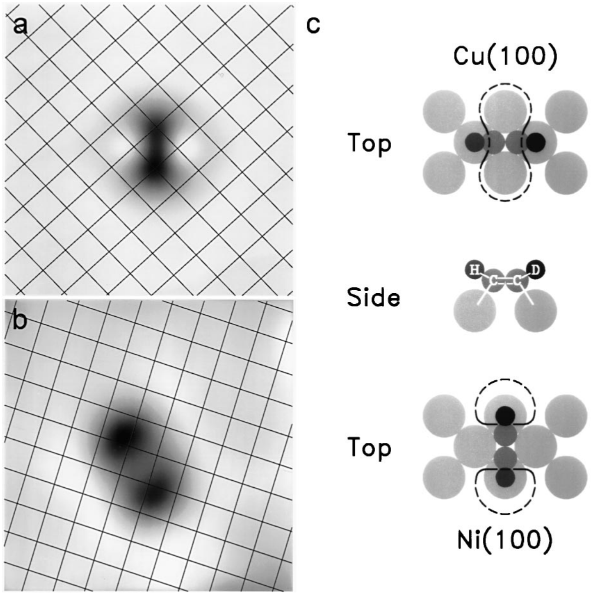

FIG. 4. STM images of acetylene on Cu(100) (a) and Ni(100) (b). The dark lobes in the images are outlined in the schematic drawings in (c). The imaged areas are 25 Å × 25 Å and were scanned at a sample bias voltage of 100 mV and a tunneling current of 10 nA. The intersections of the square lattice in (a) represent the Cu atoms of the substrate and were taken from an atomic resolution image of the same area with the C_2H_2 molecule adsorbed on the tip. The square lattice in (b) represents the positions of the Ni atoms and was taken from atomic resolution images and comparisons with the positions of coadsorbed C impurities in the fourfold hollow sites [19]. The distance between Cu atoms is 2.55 Å while the distance between Ni atoms is 2.49 Å.

times faster than on Cu(100). Stable vibrational images of acetylene on Ni(100) have not yet been achieved because the low currents required to prevent the molecule from rotating during the scan also result in a reduction of the signal-to-noise ratio (for the same reason, vibrational imaging of the C-H stretch for C_2HD on Cu(100) was not obtained). From the double-exponential distribution of rotation times in the low current state (Fig. 3d), we can conclude that the low current state corresponds to the orientation with the tip inside the plane of the molecule. Thus, in STM images the positions of the hydrogen or deuterium atoms appear somewhat bright on Cu(100) but dark on Ni(100) (Fig. 4). This happens despite the fact that the molecule is adsorbed on the same site and with the same orientation on these two surfaces.

In the case of acetylene adsorbed on the threefold hollow sites of Pd(111), a protrusion (bright) next to a depression (dark) was observed and compared to a calculation revealing the contribution from π orbitals tilted from the surface [18]. For acetylene on Cu(100), π bonding to Cu atoms may be responsible for the dark lobes normal to the plane of the molecule (Fig. 4a). Also, the origin of the sharp contrast between the STM images of acetylene on Cu(100) and Ni(100) within the plane of the molecule could be due to the close proximity of the metal d-band to the Fermi level on Ni compared to Cu. Mixing of the Ni d-band with the molecular orbitals of acetylene may reduce the density of electron states near the Fermi level in the vicinity of the H and D, resulting in dark features.

This research was supported by the National Science Foundation under Grant No. DMR-9417866.

[1] R. J. Driscoll, M. G. Youngquist, and J. D. Baldeschwieler, Nature (London) **346**, 294 (1990).
[2] G. P. Lopinski, D. J. Moffatt, D. D. M. Wayner, and R. A. Wolkow, Nature (London) **392**, 909 (1998).
[3] J. Cerdá, M. A. Van Hove, P. Sautet, and M. Salmeron, Phys. Rev. B **56**, 15 885 (1997).
[4] L. Ruan, F. Besenbacher, I. Stensgaard, and E. Laegsgaard, Phys. Rev. Lett. **70**, 4079 (1993).
[5] B. C. Stipe, M. A. Rezaei, and W. Ho, Science **280**, 1732 (1998). An early attempt to measure inelastic tunneling with the STM was documented in D. P. E. Smith, M. D. Kirk, and C. F. Quate, J. Chem. Phys. **86**, 6034 (1987).
[6] R. C. Jaklevic and J. Lambe, Phys. Rev. Lett. **17**, 1139 (1966).
[7] B. C. Stipe, M. A. Rezaei, and W. Ho, Rev. Sci. Instrum. **70**, 137 (1999).
[8] D. Arvanitis, U. Döbler, L. Wenzel, K. Baberschke, and J. Stöhr, Surf. Sci. **178**, 686 (1986).
[9] X. F. Hu, C. J. Chen, and J. C. Tang, Surf. Sci. **365**, 319 (1996).
[10] N. J. DiNardo, J. E. Demuth, and Ph. Avouris, Phys. Rev. B **27**, 5832 (1983).
[11] N. Sheppard, J. Electron Spectrosc. Relat. Phenom. **38**, 175 (1986).
[12] Ts. S. Marinova and P. K. Stefanov, Surf. Sci. **191**, 66 (1987).
[13] D. Arvanitis, K. Baberschke, L. Wenzel, and U. Döbler, Phys. Rev. Lett. **57**, 3175 (1986).
[14] A. Baratoff and B. N. J. Persson, J. Vac. Sci. Technol. A **6**, 331 (1988); B. N. J. Persson, Phys. Scr. **38**, 282 (1988).
[15] M. A. Gata and P. R. Antoniewicz, Phys. Rev. B **47**, 13 797 (1993).
[16] B. C. Stipe, M. A. Rezaei, and W. Ho, Phys. Rev. Lett. **81**, 1263 (1998).
[17] D. P. Stevenson and J. A. Ibers, J. Chem. Phys. **33**, 762 (1960).
[18] J. C. Dunphy, M. Rose, S. Behler, D. F. Ogletree, M. Salmeron, and P. Sautet, Phys. Rev. B. **57**, R12 705 (1998).
[19] C. Klink, L. Olesen, F. Besenbacher, I. Stensgaard, E. Laegsgaard, and N. D. Lang, Phys. Rev. Lett. **71**, 4350 (1993).